Seismic Design of GRS Integral Bridge

S. YAZAKI[1], F. TATSUOKA[2], M. TATEYAMA[3], M. KODA[4], K. WATANABE[5] and A. DUTTINE[6]

ABSTRACT

The current version of the seismic design of a new bridge type, called Geosynthetic-Reinforced Soil (GRS) integral bridge, used in practice is described. This new type of bridge comprises a girder integrated to a pair of abutments (i.e., full-height rigid facings) without using bearings and a pair of approach blocks of compacted cement-mixed gravelly soil reinforced with geogrid layers connected to the facings. A seismic design method based on the pseudo-static push-over analysis of a lumped-mass frame model representing the RC members (i.e., the integrated girder and facings) is described. The most critical failure mode defined based on results from a series of model shaking table tests is the rotation of the facing, which is triggered by the passive failure in the upper part of the approach block on the passive side and the tensile rupture of the geogrid at the connection with the back face of the upper part of the facing on the active side, both caused by the lateral inertia of the girder and facings. The sub-grade reactions of the approach blocks at the back face of the facings and the subsoil at the bottom face of the footings of the facings are modeled by springs having bi-linear or tri-linear force – displacement properties upper-bounded by the passive earth pressure and bearing capacity, respectively. A working example illustrating this seismic design procedure is presented. It is shown that the GRS integral bridges that are stable when subjected to very high seismic loads equivalent to the one experienced during the 1995 Great Kobe Earthquake (so called Level 2 seismic load) can be designed.

[1 & 6] Susumu Yazaki and Antoine Duttine: Integrated Geotechnology Institute Limited, Kyoritsu Yotsuya Building, 1-23-6 Yotsuya, Shinjuku-ku, Tokyo, 160-0004, Japan

[2] Fumio Tatsuoka: Tokyo University of Science, 2641 Yamazaki, Noda, Chiba, 278-8510, Japan

[3-5] Masaru Tateyama, Masayuki Koda and Kenji Watanabe: Railway Technical Research Institute, 2-8-38 Hikari-cho, Kokubunji, Tokyo, 185-8540, Japan

INTRODUCTION

The conventional type bridge has a number of inherent problems due to its structural features (i.e., the girder is placed on the top of the abutments via a pair of bearings and the backfill is not reinforced) and its specific construction procedure (i.e., the approach backfill is constructed retained by abutments that have been constructed) [1 – 3]. To alleviate these problems, other than those due to the use of bearings, a new type bridge abutment described in Fig. 1 was developed. For this type of bridge abutment, a geosynthetic-reinforced soil (GRS) retaining wall not having a full-height rigid (FHR) facing is first constructed. After the deformation of the subsoil and the backfill due to the construction of the GRS wall, a FHR facing is constructed in such that it is firmly connected to the geogrid reinforcement layers at the wall face. Finally, the girder is placed on the top of the facing via a bearing (usually a fixed one comprising a pin).

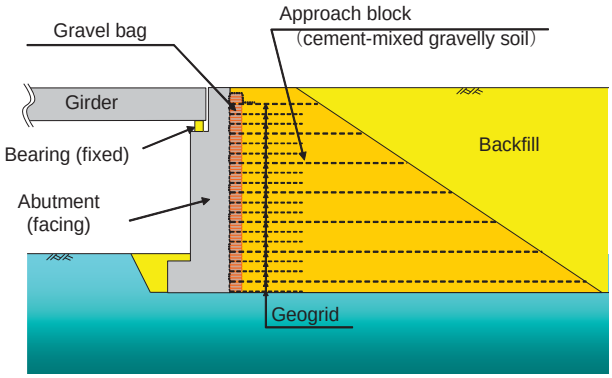

Figure 1. GRS bridge abutment [4, 5]

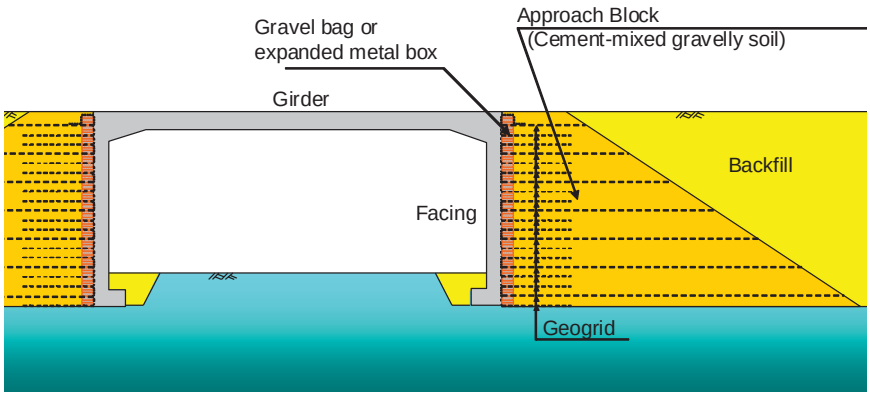

Figure 2. GRS integral bridge [2-4, 5]

To alleviate several problems due to the use of bearings with the GRS bridge abutment (Fig. 1), the GRS integral bridge (Fig. 2) was developed [2-4, 5]. A continuous girder is integrated without using bearings to the top of a pair of the FHR facings of GRS walls. In the beginning of 2009, a full-scale GRS bridge model (Figs. 3 & 4) was constructed [6]. Koda et al. [7, this conference] reports results of lateral cyclic loading tests simulating annual thermal effects and seismic loading on this full-scale model performed in the beginning of 2012, after having monitored the behaviour of the model for two years. In 2012, the first prototype

GRS integral bridge, for a new high-speed train line called Hokkaido Shinkansen, was completed [8]. Presently (June 2013), three more GRS integral bridges are under construction to restore two bridges and an elevated RC frame structure that fully collapsed by tsunami during the 2011 Great East Japan Earthquake [3, 5, 9]. These four GRS integral bridges were designed referring to the design codes for GRS abutments (Fig. 1) [10, 11]. Based on these experiences, the draft of the seismic design code for GRS integral bridges is currently under preparation.

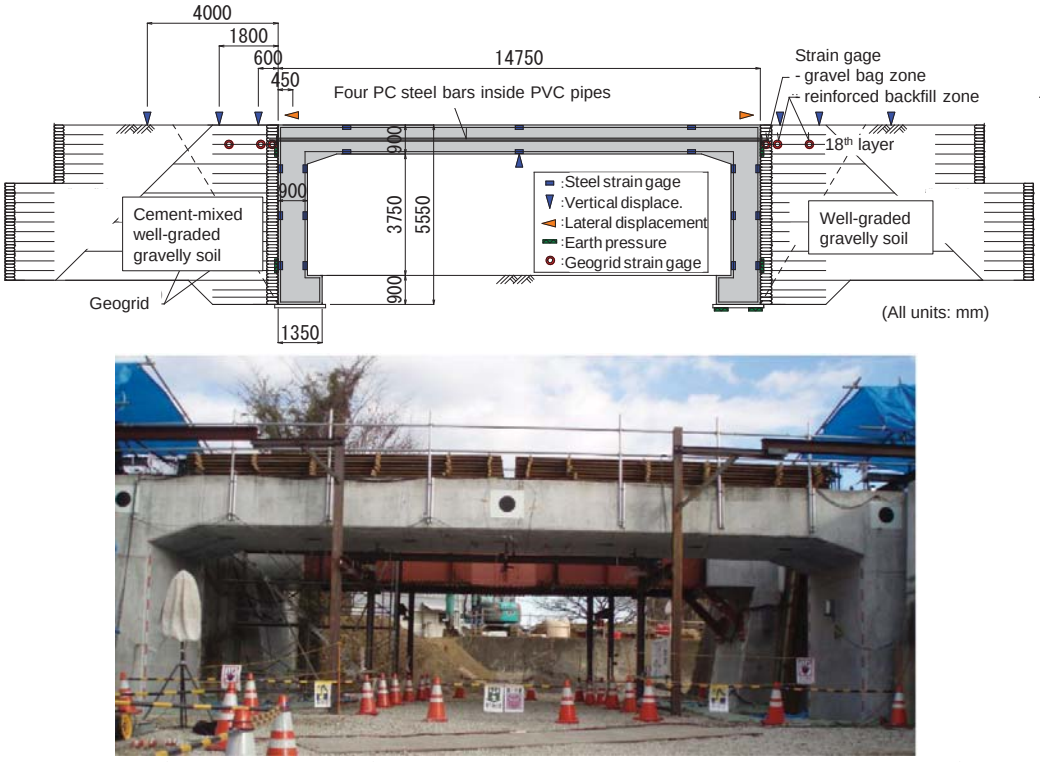

Figure 3. A full-scale model of GRS integral bridge completed in the beginning of 2009 (this picture was taken during lateral cyclic loading tests in the beginning of 2012).

In this paper, the current version of the seismic design, by which the four prototype GRS integral bridges were designed, is described. As a working example, the seismic design of the full-scale model (Fig. 3) is presented. The stability of the bridge against seismic loads activated in the bridge axial (longitudinal) direction, which is more critical in ordinary cases, is examined. The stability in the transversal direction, which becomes more important as the ratio of the girder length to the girder width increases, will be reported elsewhere.

SEISMIC DESIGN METHODOLOGY

Basic concept

Fig. 4 summarizes the components of load and resistance taken into account and the damage and failure modes examined in the current version of the seismic design of GRS integral bridges in the case where lateral seismic loads are activated in the longitudinal bridge axis direction. It is naturally assumed that the seismic

response of the RC members (i.e., the girder and facings) is larger than that of a pair of approach blocks comprising compacted cement-mixed gravelly soil on both sides, while the seismic response of the backfill in back of the approach block on the active side is larger than the approach blocks. Then, the seismic load components to be taken into account are as follows:

1) The inertia of the RC members, which is transmitted to the approach block on the passive side mainly via lateral compression loads (i.e., the passive earth pressure) and to the approach block on the active side mainly via tensile forces in the geogrid at the connection to the facing.
2) The inertia of the approach block on the active side together with the back-side backfill overlying this approach block, which is applied to the approach block on the active side.
3) The seismic active earth pressure activated to the virtual vertical wall face in back of the approach block on the active side.

In laboratory model shaking table tests [1], the inertia of the RC members is resisted by the approach fills on both sides and the most critical failure/collapse mode is the rotation of the facing that is triggered by the passive failure in the upper part of the approach block on the passive side caused by the lateral inertia of the girder and facings. Unlike the laboratory model tests, in which the approach fills were air-dried Toyoura sand, in the case analyzed in this paper, the approach fills are compacted cement-mixed gravelly soil (called the approach blocks), which are much more stable than the approach fills in the laboratory model tests. It is considered that, in this case, the rotation of the facing is triggered also by the tensile rupture of the geogrid at the connection at the back face of the upper part of the facing on the active side and/or shear failure inside the approach block on the active side. A large rotation of the facing eventually results in the collapse of the bridge with a significant decrease in the distance between the footings of the facings on both sides. This mode is due to large active pushing out of the footing on the passive side associated with the tensile rupture of the geogrid at the connection to the lower part of the facing. When the RC members are not strong enough, they may be seriously damaged during this process. In the design, it is examined whether the RC members and approach blocks can maintain their stability under such loading conditions as above.

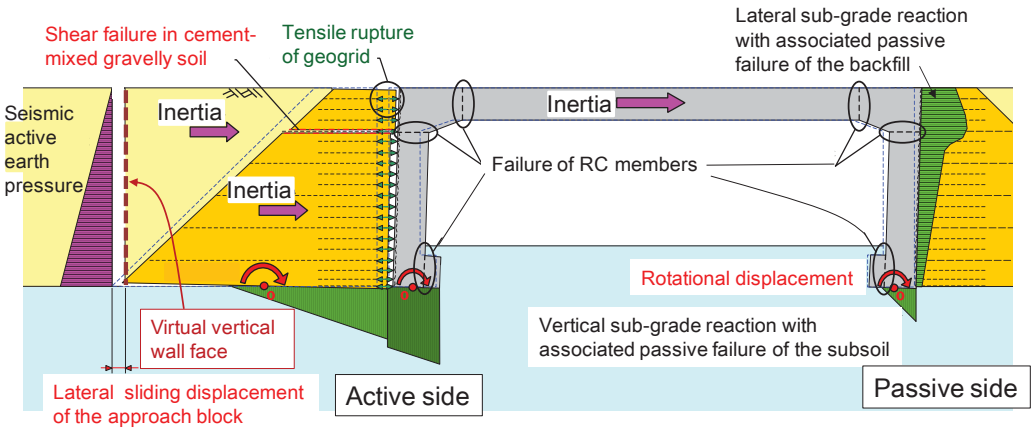

Figure 4. Load & resistance components and damage & failure modes in the seismic design of GRS integral bridge.

It is assumed that the horizontal seismic coefficient, k_h, used to obtain the inertial of the RC members in the pseudo-static stability analysis is equal to the peak horizontal acceleration on the ground surface, α_{max}, divided by g (the gravitational acceleration) (i.e., $k_h = \alpha_{max}/g$). It is considered that this approximation is reasonable as a whole for the following reasons. Firstly, this approximation is conservative in that, in actuality, the peak acceleration is activated temporarily one time, not as assumed in the pseudo-static stability analysis. Secondly, this approximation is un-conservative in that, in actuality, the ratio of the response acceleration at the girder to the acceleration on the ground surface, *M*, is larger than unity, unlike this approximation. It is considered, however, that the value of *M* during severe earthquakes would not become considerably higher than unity. This is because, in the results of shaking table tests [1, 12], the *M* value was only around 1.4 even when failure started at the resonance state. This was due to the following mechanisms, all due to a very high structural integrity of GRS integral bridges:

1) The initial *M* value when the input acceleration is low is controlled by the initial value of the natural frequency (f_0) of a given GRS integral bridge relative to the predominant frequency of a given design seismic load (f_i). The largest *M* value is obtained at the resonance when the ratio, f_i/f_0, is slightly lower than the unity. The vibration test of the full-scale GRS integral bridge model showed the initial value of f_0 is 21.7 Hz [14], which is much larger than f_i values of strong seismic motions, around 1- 2 Hz. Therefore, the initial value of f_i/f_0 is substantially smaller than unity, which results in a very low initial value of *M*, close to unity.

1) With an increase in the seismic load, the stiffness of the bridge decreases, therefore, f_o decreases. As the decreasing rate of f_0 during seismic loading is substantially lower than the conventional type bridges and not large, the ratio f_i/f_0 could be kept to be much lower than unity maintaining the dynamic behaviour of the bridge far remote from the resonance state.

2) As a good contact between the facings and the approach blocks and subsoil is maintained, the capacity of dissipating the dynamic energy of the RC members (in particular, that of the girder) to the approach blocks and the subsoil is kept very high. Therefore, the damping ratio of the bridge as a lumped mass is very high.

The interaction (i.e., changes in the forces activated at the boundary between a given structure and the surrounding soil mass) by seismic loads is insignificant with such under-ground structures as tunnels. On the other hand, the interaction is significant with shallow foundations for a massive superstructure extruding above the ground surface (such as shallow foundations for piers of a bridge). It is assumed that the interaction between the RC members of GRS integral bridge and the approach blocks and subsoil is similar as the latter case, that is, the inertial of the RC members obtained by the k_h value defined above is fully supported by changes in the forces activated at the boundary between the RC members and the approach blocks and subsoil. This is a very conservative approximation for the evaluation of these boundary forces. The same conservative approximation was adopted in lateral cyclic loading tests simulating seismic loading on the full-scale model (Fig. 3; [7]).

The stability of GRS integral bridge is controlled by the dimensions of the major structural components (i.e., the girder, facing and approach blocks) and their properties: i.e., the strength and stiffness of: 1) the girder and facings; 2) the geogrid reinforcement at and around the connections to the facing and the geogrid in the pull-out mode; 3) the approach blocks in the active and passive modes; 4) the stability of the backfill in back of the approach blocks; and 5) the subsoil. Taking into account these factors listed above, the response of the GRS integral bridge when subjected to the seismic loads (explained above) is evaluated by the following two steps of analysis assuming different conditions with respect to deformations and displacements of the approach blocks relative to the subsoil, as follows:

Analysis I: Evaluation of forces in the RC members and boundary forces by not considering deformation of the approach blocks and their displacements relative to the subsoil: It is assumed that the approach blocks are internally and externally very stable under specified seismic loading conditions explained above, exhibiting no internal failure and no displacements relative to the subsoil. The following responses and possible associated damage/failure of the RC members and the subsoil supporting the footings of the facings are examined:

(1) Vertical sub-grade reaction at the base of the footings of the facings on the active and passive sides, which is upper-bounded by the bearing capacity of the subsoil.
(2) Lateral sub-grade reaction at the interface between the facing and the approach blocks on both sides (in particular at the upper part of the passive side facing), which is upper-bound by the passive yield strength (i.e., the allowable passive earth pressure).
(3) Geogrid tensile forces at the connections on the back of the facing of the approach blocks on both sides (in particular at the upper part of the active side facing), which is upper-bound by the tensile rupture strength of the geogrid.
(4) Internal forces in the RC members to examine whether large-scale yielding that seriously damage them takes place.

These items are evaluated by a pseudo-static pushover analysis of the lumped mass frame model illustrated in Fig. 5. When the lateral load at the back of the facing is in compression, the springs representing the lateral sub-grade reaction of the approach block work, while the lateral load is in tension, the springs representing the geogrid properties at the connection work.

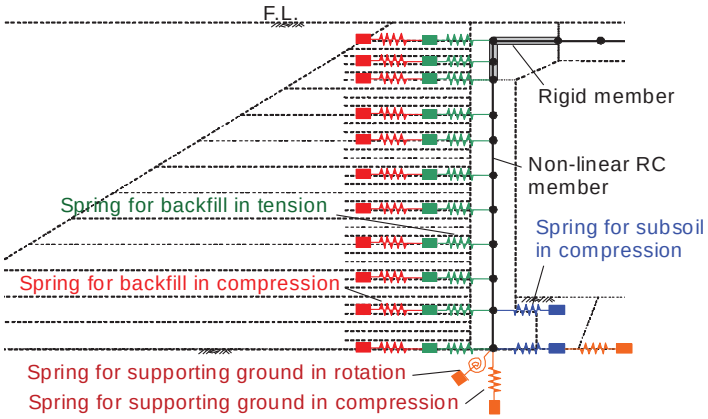

Figure 5. Two-dimensional lumped-mass frame model of the active and passive sides of GRS integral bridge for quasi-static non-linear analysis (analysis I)

Analysis II: Evaluation of the deformation of the actove side approach block and its displacements relative to the subsoil: As more realistic analysis, it is considered that the approach block on the active side exhibits internal deformation and relative displacements under specified seismic loading conditions. To evaluate the internal and external stability of the approach block, the same design horizontal seismic coefficient k_h as the one applied to the RC members in analysis I is applied to the approach block on the active side and the over-lying backfill. As a conservative approximation, the tensile forces at the back of the facing on the active side evaluated by analysis I are also used in analysis II. The following responses and possible associated damage/failure of the approach blocks are evaluated and examined:

(5) Vertical sub-grade reactions at the base of the approach block on the active side, which is upper-bounded by the bearing capacity of the supporting ground.

(6) Lateral sliding of the approach block on the active side along the interface with the subsoil. The model depicted in Fig. 6 is used to examine terms (5) and (6).

(7) Internal forces in the approach blocks to examine whether the internal failure takes place in the approach blocks on the active side. The model depicted in Fig. 7 is used to examine whether sliding takes place along the horizontal plane inside the approach block exhibiting the minimum safety factor.

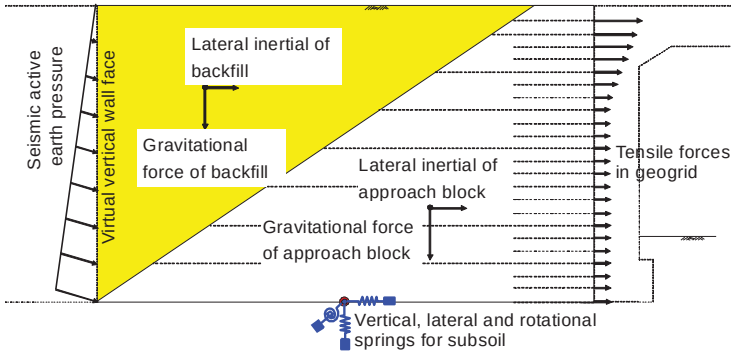

Figure 6. Evaluation of the external stability of the approach block on the active side (analysis II)

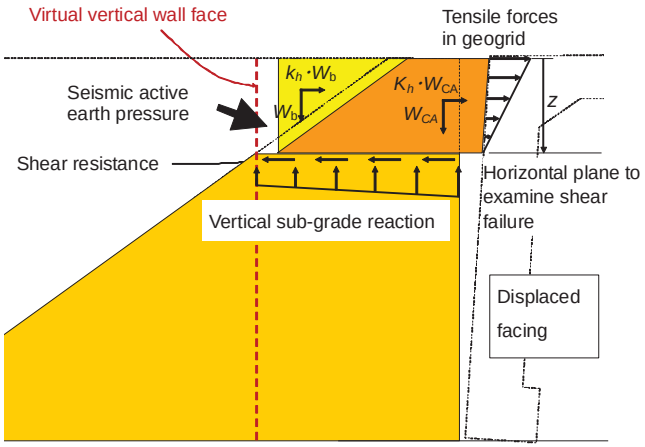

Figure 7. Evaluation of the internal stability of the approach block on the active side (analysis II)

WORKING EXAMPLE

The dimensions of the full-scale model (Fig. 3) were determined referring to the ordinary RC frame structure for an elevated railway. In this section, the seismic design procedure of a GRS integral bridge is described by showing the design of the GRS integral bridge presented in Fig. 8, which is very similar to the full-scale model presented in Fig. 5.

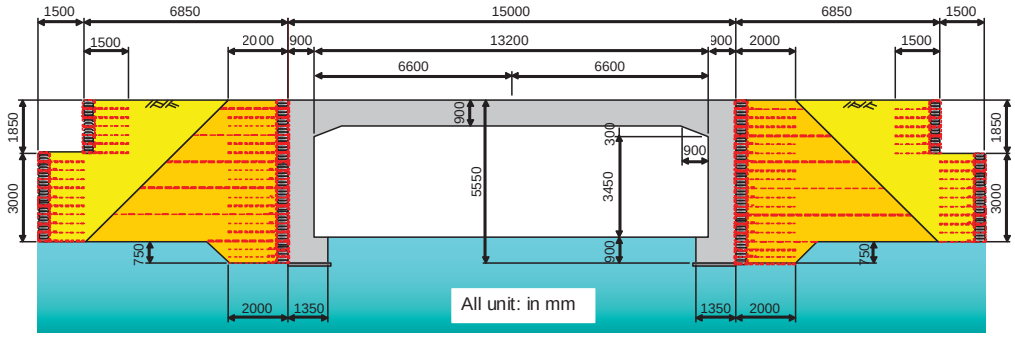

Figure 8. GRS integral bridge designed in this study (width= 3.0 m)

Design conditions

1) General structure (Fig. 8)
   a) RC members (i.e., a girder and a pair of FHR facing): Unlike the full-scale model (Fig. 3), the approach blocks on both sides comprise compacted cement-mixed well-graded gravelly soil.
   b) Geogrid reinforcement: The basic length of the geogrid that reinforces the backfill of the approach blocks is equal to 2.0 m, determined following the specification of geosynthetic-reinforced soil retaining walls having FHR facing [1, 11] that "*the minimum length is the larger one of 35 % of the wall height, which is equal to 5.55 m × 0.35= 1.94 m in this case, and 1.5 m*". Also following the same specification, the vertical spacing of geogrid layers was determined to be 30 cm. For satisfactory monolithic behavior of the approach block, one of every there layers was made long enough to reach the back end of the approach block. Several other assumed key properties of the geogrid are listed in Table 1. The tensile stiffness of geogrid, often called the spring constant, is the value for a geogrid specimen with a length of 40 cm, which is equal to the width of gravel bags between the facing and the approach block of cement-mixed GS in the present case. The stiffness value when placed in air is due solely to the stiffness of geogrid, while the value when placed in the gravel bag zone was then one measured by lateral pull-out tests of the geogrid performed at the first prototype GRS bridge abutment (Fig. 1) constructed at Takada for Kyushu Sinkansen [10].

Table 1 Design properties of the geogrid

Material	Tensile rupture strength（kN/m）	Tensile stiffness for a length of 40 cm (kN/m/m） when placed:	
		In air	In the gravel bag zone
Polyvinyl alcohol (PVA) fibre covered with polyvinyl chloride (PVC).	59	490	2,450

c) Subsoil and backfill: The assumed subsoil is a stable sandy soil deposit exhibiting a blow count by the standard penetration test equal to, or more than, 50, having the properties listed in Table 2. The assumed backfill has well-graded gravelly soil having the properties listed in Table 3.

Table 2 Design properties of the supporting ground

Soil type	SPT N value	Total unit weight, γ（kN/m^3）	Friction angle, φ（°）	Cohesion intercept, c（kN/m^2）
Sandy gravel including clay	≧50	20	43	0

Table 3 Design properties of the backfill

Soil type	Total unit weight, γ（kN/m^3）	Residual angle, φ_{res}	Peak angle. φ_{peak}
(Soil type 1): Well-graded gravelly soil	20	40°	55°

d) Cement-mixed gravelly soil: The design properties of the original gravelly soil are the same as the ones listed in Table 3 and those of compacted cement-mixed gravelly soil are listed in Table 4.

Table 4 Design properties of cement-mixed gravelly soil

Item	Design value	Note
Unit weight	γ= 20 kN/m^3	
Unconfined compression strength	q_u = 2.0 MPa	
Tensile strength	$\sigma_c = \frac{q_u}{10} = 0.2$MPa	
Stiffness	$E_{50} = 200q_u = 400$ MPa	
Peak strength parameters	c =315 kN/m^2, φ_{peak}= 55° $\left(c = \frac{q_u(1-\sin\phi_{peak})}{2\cos\phi_{peak}} = 315\text{kN/m}^2 \right)$	φ_{peak} is the value of the original well-graded gravelly soil. Cohesion intercept c is due to bond strength of cement
Residual strength parameters	c = 0 kN/m^2, φ_{res} = 40°	φ_{res} is the value of the original well-graded gravelly soil. c = 0 due to severe damage to bonding at the residual condition

2) Seismic design procedure

The terms to be examined in the seismic design are listed in Table 5. In the following, analysis I of these items using the model illustrated in Fig. 5 is described.

Table 5 Items to examine for seismic design

Mode	Structural member	Item to be examined
Overall stability	Footing of the facing	Rotational and lateral displacements at the interface with the subsoil due to the bearing capacity failure of the subsoil
	Approach block	

Damage/failure	RC members	Yielding in the bending mode and the associated amount of curvature and flexural deformation
	Geogrid	Tensile rupture determined by comparing developed tensile strains with the value at rupture
	Approach block	Yielding in the modes of bending, shear and compression

3) Analysis model

The behaviour of a lumped-mass frame model discretized into 57 nodes and 56 elements (Figs. 9a & b) of the RC members (i.e., the girder and facings) was analysed. The hunch section at the girder/facing connection on each side was modelled as a rigid element. The other elements exhibit tetra-linear force-deformation properties as seen from Fig. 14 (shown later).

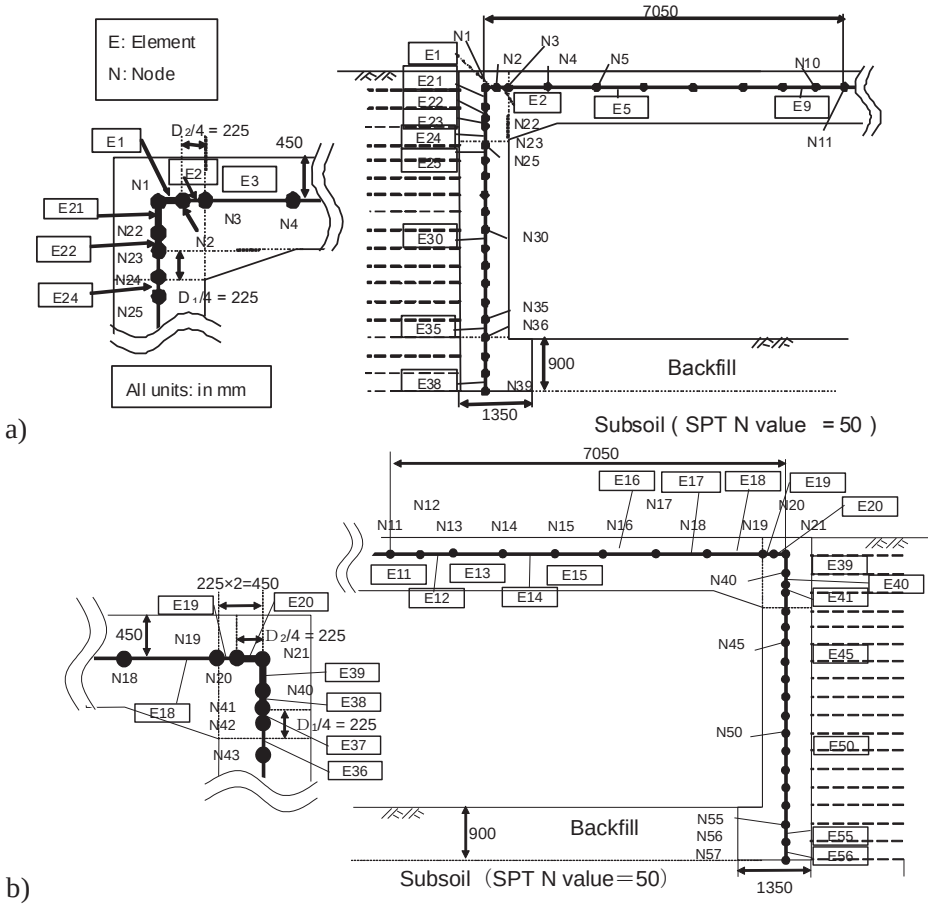

a)

b)

Figure 9. Lumped-mass frame models for the RC members on: a) the active side; and b) the passive side.

The vertical, horizontal and rotational subgrade reactions at the boundary between the RC members and the approach blocks or subsoil were modelled by springs as shown in Fig. 10. The force – displacement properties of the springs are explained in Table 6. The tensile resistance of the geogrid at the back face of the facing was represented by a bi-linear model upper-bound by the design rupture strength (Table 1) while exhibiting no resistance against compression.

Table 6 Non-linear properties of springs representing the sub-grade reactions

Subgrade type and working direction		Non-linearity model	Effective condition
Backfill	Horizontal	Bi-linear (linear – perfectly plastic)	Compression only
Subsoil	Horizontal	Bi-linear	Both horizontal directions
	Vertical	Bi-linear	Compression only
	Rotational	Tri-linear	Both directions of rotations

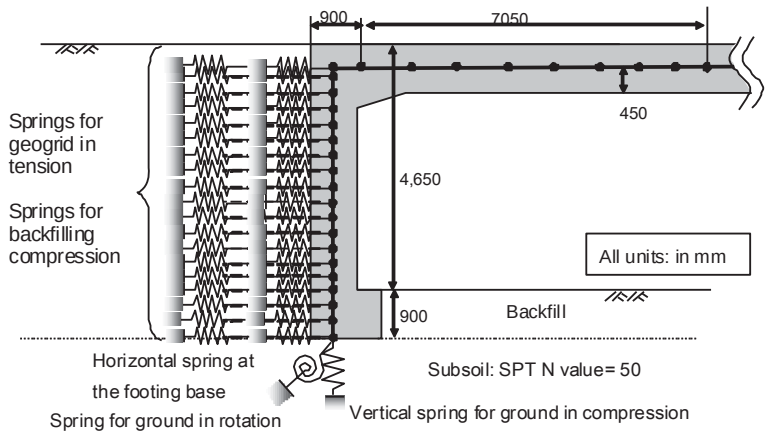

Figure 10. Springs at the boundary between the RC members and the approach block and subsoil (corresponding to Fig. 5).

The self-weight of the RC members (fixed values) was distributed to the nodes shown in the models (Figs. 9a & b). The behaviour of the model was analysed by means of push-over analysis applying the inertia of the RC members to the respective nodes incrementally by 1,000 steps until the horizontal seismic coefficient k_h became 1. 0 (i.e., the gravitational acceleration, 1g). According to the seismic design code for railway structures [13], the value of $k_h = \alpha_{max}/g$ for L2 seismic design load is very high, equal to 871/980= 0.889 for the subsoil condition (so-called G2 type) in the present design case.

Results of design analysis

Fig. 11 shows the displacements of the RC members and the internal forces developed in the RC members when k_h= 1.0 obtained by the push-over analysis. The largest lateral displacement is about 8.5 mm and the largest vertical displacement is about 11.5 mm.

Figs. 12 shows the relationship between the horizontal seismic coefficient, k_h, and the lateral displacement at node No. 4 (at the top end of the hunch at the girder/facing connection on the active side, Fig. 9a) until k_h becomes 1.0. As a set of springs from node No. 21 and then from node Nos. 41 through 48 on the back of the facing on the passive side reach the respective yield points (i.e., the earth pressure reaches the passive earth pressure), the relation becomes more non-linear exhibiting lower tangent stiffness. The spring at node No. 48, located below the hunch, reached the yield point immediately before step No. 1,000, at which k_h becomes 1.0.

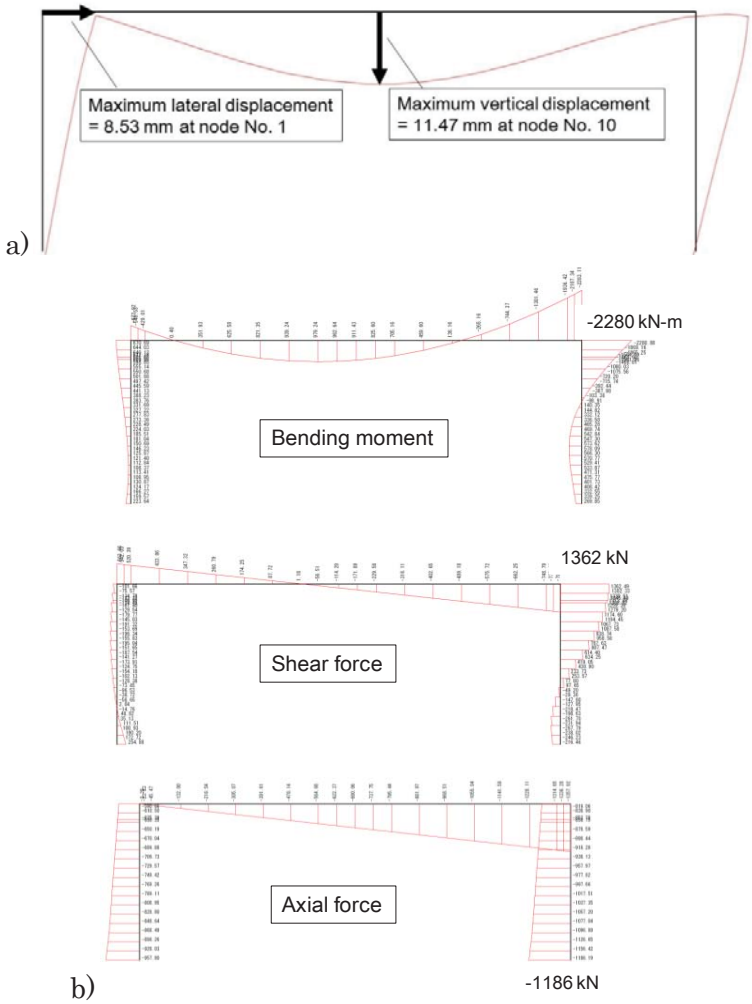

Figure 11. Displacements of the RC members; and b) internal forces for a 3 m-width in the RC members when k_h= 1.0 by the push-over analysis

Figs. 13a & b show the relationships between the bending moment (for a width of 3 m) and the rotational displacement at the center of the base of the footing of the facing on the active side (Fig. 9a) and the passive side (Fig. 9b) until k_h becomes 1.0. It is assumed that the properties of the rotational spring do not change after the toe of the footing base starts separating from the subsoil. This moment is denoted M1 in these figures. It may be seen that the state M1 is reached before k_h becomes 1.0. Yet, the allowable limit at which the whole of the footing base has separated from the subsoil is not reached.

The reacting vertical contact forces for a width of 3 m, V_d, at the footing base of the footings on the active and passive sides when k_h becomes 1.0 were both substantially lower than the respective bearing capacities, R_{vd}, as follows:

Active side: V_d= 958.0 kN ≦ R_{vd}= 2136.6 kN

Passive side: V_d=1186.0 kN ≦ R_{vd}= 2356.4 kN

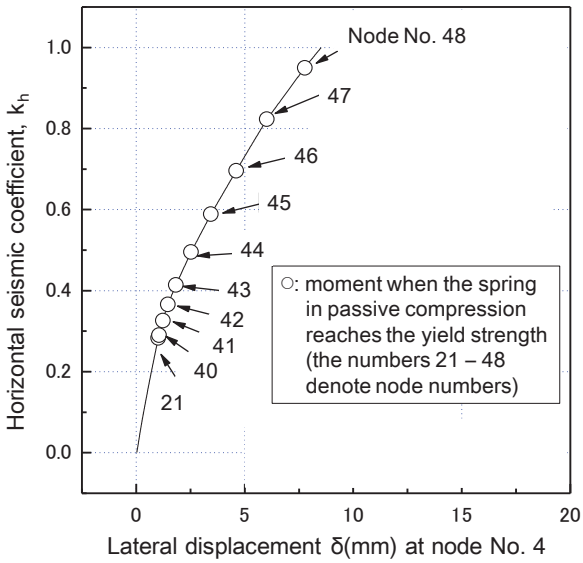

Figure 12. Horizontal seismic coefficient – lateral displacement at node No. 4 (at the hunch at the girder/facing connection on the passive side, Fig. 9a).

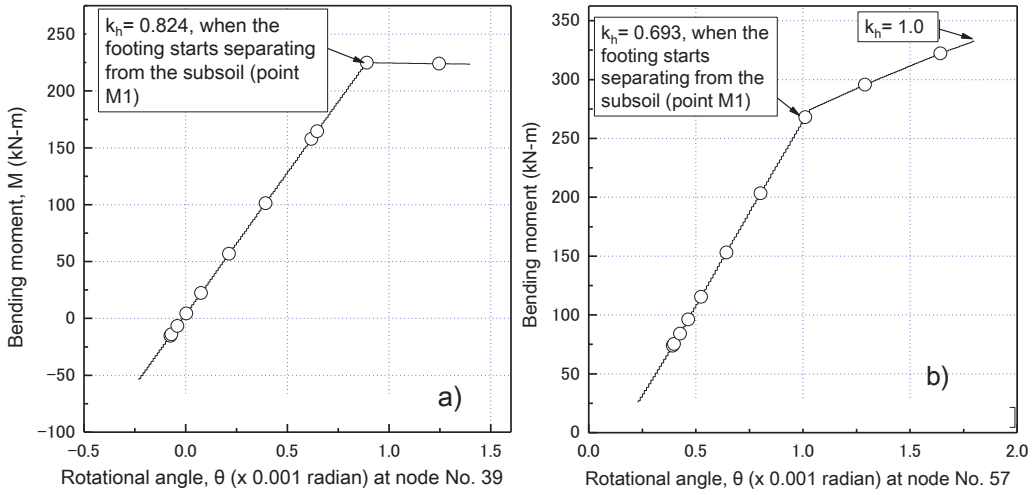

Figure 13. Bending moment – rotational displacement relation at the base of the footing of the facing on: a) the active side (Fig. 9a); and b) n the passive side (Fig. 9b).

Figs 14a – c show the relationships between the bending moment, *M*, for a width of 3 m and the curvature, φ, at three representative locations in the RC members. In each figure, the moment when the k_h value reaches 1.0, which exceeds the specified L2 seismic load level (i.e., k_h= 0.889), is indicated. It may be seen that, even by applying such a high level of seismic load, the large-scale yielding has not yet started. It was confirmed that it is also the case with all the other elements. These results indicate that it is quite feasible to design GRS integral bridges that can withstand such very high seismic load as L2 design seismic load at a cost that is substantially lower than conventional type bridges having a similar level of seismic stability.

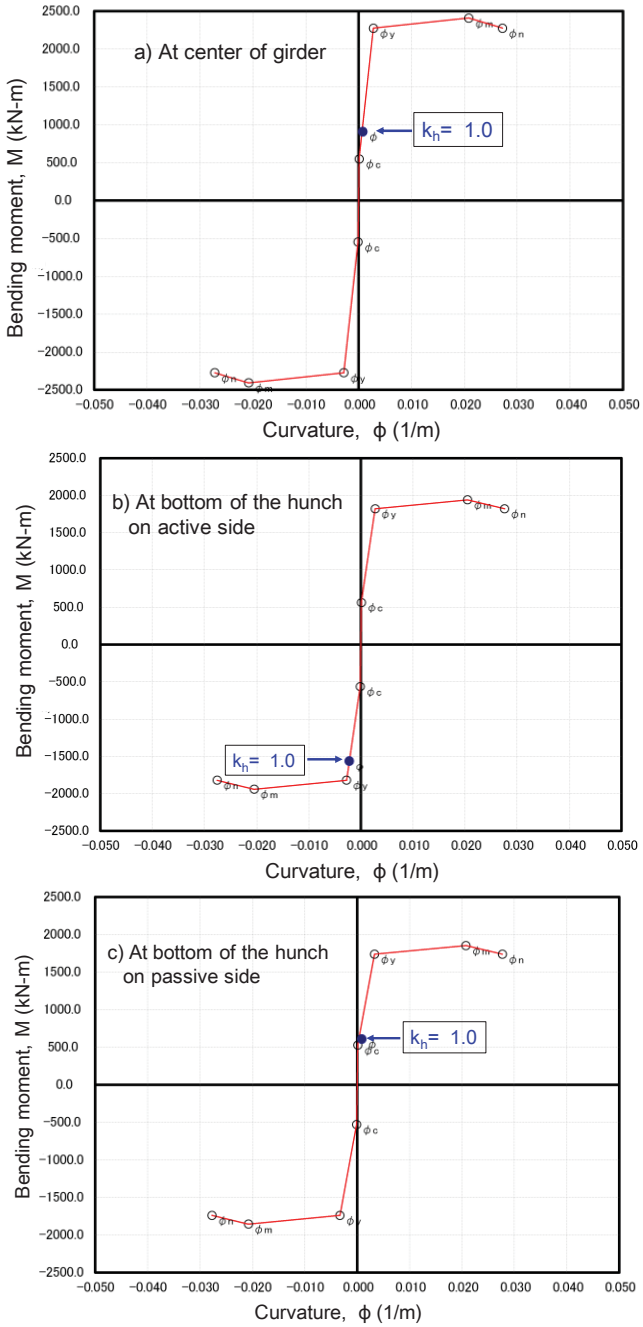

Figure 14. Bending moment – curvature relations at representative locations.

CONCLUDING REMARKS

The basic concept and a working example of the seismic design of the GRS integral bridge was described in this paper. So far, one full-scale model and four prototypes were designed based this practical method.

The seismic design method described in this paper is consistent with the results of the loading tests of the full-scale model (Fig. 3), reported by Koda et al. [5], in that the GRS integral bridge analyzed and tested could withstand Level 2 design

seismic load, not damaged to the level requiring repair works. Currently, the relevance of the seismic design method described in this paper is being examined in details by compared with the results of the loading tests of the full-scale model. Based on these analyses, the first draft of the seismic design code will then be prepared.

REFERENCES

1. Tatsuoka, F., Tateyama, M, Uchimura, T. and Koseki, J. 1997. "Geosynthetic-reinforced soil retaining walls as important permanent structures", *Mercer Lecture, Geosynthetic International*, Vol.4, No.2, pp.81-136.
2. Tatsuoka, F., Hirakawa, D., Nojiri, M., Aizawa, H., Nishikiori, H., Soma, R., Tateyama, M. and Watanabe, K. 2009. "A new type integral bridge comprising geosynthetic-reinforced soil walls", *Gesynthtetics International, IS Kyushu 2007 Special Issue*, 16(4): pp.301-326.
3. Tatsuoka, F., Tateyama, M. and Koseki, J. 2012. "GRS structures recently developed and constructed for railways and roads in Japan", Keynote lecture, *Proc. 2nd International Conference on Transportation Geotechnics (IS-Hokkaido 2012)* (Miura et al., eds.), pp.63-84.
4. Yonezawa, T., Yamazaki, T., Tateyama, M. and Tatsuoka, F. 2013. "Various geosynthetic-reinforced soil structures for Hokkaido high-speed train line", *Proc. International Symposium on Design and Practice of Geosynthetic-Reinforced Soil Structures, Oct. 2013, Bologna* (Ling et al., eds.) (this conference).
5. Koda, M., Nonaka, T., Suga, M., Kuriyama, R, Tateyama, M. and Tatsuoka, F. 2013. "Lateral cyclic loading tests of a full-scale GRS integral bridge model", *Proc. International Symposium on Design and Practice of Geosynthetic-Reinforced Soil Structures, Oct. 2013, Bologna* (Ling et al., eds.) (this conference).
6. Tatsuoka, F., Tateyama, M., Koseki, J. and Yonezawa, T. 2013. "Geosynthetic-reinforced soil structures for railways twenty five year experiences in Japan", *Geotechnical Engineering Journal of the SEAGS & AGSSEA* (to appear).
7. Aoki, H., Yonezawa, T., Tateyama, M., Shinoda, M. & Watanabe, K. 2005. "Development of a seismic abutment with geogrid-reinforced cement-treated backfill", *Proc. 16th IC on SMGE, Osaka*, pp.1315-1318.
8. Tatsuoka, F., Tateyama, M., Aoki, H. and Watanabe, K. 2005. "Bridge abutment made of cement-mixed gravel backfill", *Ground Improvement, Case Histories, Elsevier Geo-Engineering Book Series, Vol. 3* (Indradratna & Chu eds.), pp.829-873.
9. Nagatani, T., Tamura, Y., Iijima, M., Tateyama, M., Kojima, K. and Watanabe, K. 2009. "Construction and field observation of the full-scale test integral bridge", *Geosynthetics Engineering Journal*, Vol.24, pp.219-226.
10. Railway Construction Headquarters, Japan Railway Construction, Transport and Technology Agency 2004. "Specifications for design and construction of bridge abutments comprising cement-mixed backfill", February (in Japanese).
11. Railway Technical Research Institute, 2012. "Design standard of soil retaining structures for railway structures", January, *Maruzen*, pp.297-314 (in Japanese).
12. Munoz, H., Tatsuoka, F., Hirakawa, D., Nishikiori, H., Soma, R., Tateyama, M. and Watanabe, K. 2012. "Dynamic stability of geosynthetic-reinforced soil integral bridge", *Gesynthtetics International*, Vol.19, No.1, pp.11-38.
13. Railway Technical Research Institute, 1999. "Seismic design standard for railway structures", *Maruzen*, p.65 (in Japanese).
14. Yokoyama, T., Koda, M., Tateyama, M., Kuriyama, R., Suga, M. and Nonaka, T. 2012. "Vibration tests of full-scale GRS integral bridge model", *Proc. Annual Symposium of 67th Japanese Society for Civil Engineers*, September, Paper No.III-294, pp.589-590 (in Japanese).